# BEACH PROFILE EVOLUTION IN FRONT OF STORM SEAWALLS: A PHYSICAL AND NUMERICAL STUDY

Saponieri, A. [1], Di Risio, M. [2], Pasquali, D. [3], Valentini, N. [4], Aristodemo, F. [5], Tripepi, G. [6], Celli, D. [7], Streicher, M. [8], Damiani, L. [9]

Large-scale physical experiments (Froude scale, 1:4.3) were performed at the new Delta Flume in 2017, aimed at investigating wave impacts on a vertical wall placed on the top of a dike in a mild slope shallow foreshore. Experiments also allowed to investigate the morphological evolution of the sandy foreshore, the scour at the dike toe and its development under irregular and bi-chromatic wave conditions. Both experimental results and numerical study performed to design the experiments are reported. Moreover, preliminary validation of the model to investigate the scour within a wider range of wave conditions and foreshore slopes is illustrated.

*Keywords: dike; seawall; bed scour; XBeach; beach morphodynamics.*

## INTRODUCTION

Urban development along the European coast led to a new definition of waterfronts which are now becoming a driver of cities development, with special attractiveness for urban housing, workplaces and recreation. Coastal zones are therefore facing fast population growth and urbanization.

Accordingly, reliable guidance for management of coastal defences are required, aimed at mitigating and preventing flood risk (Di Risio et al., 2017; Valentini et al., 2017), by increasing resilience of infrastructures and people (e.g., Pagano et al., 2018) as well and exposure to overtopping, also exacerbated by climate changes. As highlighted in Allsop et al. (2008), direct wave and overtopping effects are not only related to hazard to economic and environmental resources, but also to both long and short term damage to defence structures, which could lead to breaching and flooding as well.

In particular, information on the behaviour of scour in front of sea walls has great practical and theoretical interest, since erosion at the toe of foundation is one of the direct cause of the collapse of the structure (Celli et al., 2018). In literature, most empirical-based formulas on scour at coastal structures (in general, pipelines, vertical breakwaters and rubble mound breakwaters) refer to non-breaking regular waves and no-suspension mode of sand transport (e.g., De Best and Bijker, 1971; Xie, 1981; Fowler et al., 1992; Sumer and Fredsøe, 2000).

Recently, different scenarios have been investigated, dealing with an inclined concrete wall representing the dike, frequent occurrence of breaking waves, suspension mode of sediments and presence of very shallow to extremely shallow foreshore (e.g., Tsai et al., 2009; Chen et al., 2015; Altomare et al., 2016; Chen et al., 2016). In such a context, the classification of foreshore plays a relevant role, also intimately related to the intensity of storm surges (e.g. Pasquali et al., 2015). Indeed, the typical spectral shape, flat or double-peaked depth-dependent and the predominance of low-frequency waves influence the definition of wave bulk parameters and the estimates of quantities related to many processes (e.g., run-up and overtopping volumes).

New large-scale physical experiments on movable-bed (Froude scale, 1:4.3) were performed at the new large-scale Delta Flume in Delft (The Netherlands), mainly aimed at investigating overtopping wave impacts on storm walls and buildings placed on the top of a dike in mildly sloping shallow foreshore conditions (WAve LOads on WAlls - WALOWA, Streicher et al., 2017). Previous small-scale experiments were performed on a fixed bed (e.g. Chen et al., 2015, 2016; Altomare et al., 2016) thus allowing the

[1]Department of Civil, Environmental, Building Engineering and Chemistry, Politecnico di Bari, Italy, alessandra.saponieri@poliba.it

[2]Department of Civil, Construction-Architectural and Environmental Engineering, Environmental and Maritime Hydraulic Laboratory (Llam), Italy, marcello.dirisio@univaq.it

[3]Department of Civil, Construction-Architectural and Environmental Engineering, Environmental and Maritime Hydraulic Laboratory (Llam), Italy, davide.pasquali@univaq.it

[4]Department of Civil, Environmental, Building Engineering and Chemistry, Politecnico di Bari, Italy, nico.valentini@poliba.it

[5]Department of Civil Engineering, University of Calabria,Italy, francesco.aristodemo@unical.it

[6]Department of Civil Engineering, University of Calabria, Italy, giuseppe.tripepi@unical.it

[7]Department of Civil, Environmental, Building Engineering and Chemistry, Politecnico di Bari, Italy, daniele.celli@poliba.it

[8]Department of Civil Engineering, Ghent University, Technologiepark 904, B-9052 Zwijnaarde (Ghent), Belgium, maximilian.streicher@UGent.be

[9]Department of Civil, Environmental, Building Engineering and Chemistry, Politecnico di Bari, Italy, leonardo.damiani@poliba.it

analysis of wave forces and overtopping, by neglecting the effects of beach morphological evolution on both wave propagation and impact on structures.

WALOWA tests represent a novelty in the field of morphodynamic effects near coastal structures and qualitative features and trends could be interesting due to the large scale of the experimental investigation. The new experiments were performed on a mild slope shallow sandy foreshore. Besides the study of wave impact forces and pressures on the wall, tests also allowed to observe the morphological evolution of the cross-shore beach profile under irregular and bi-chromatic wave attacks and various water levels.

In the present paper, foreshore morphological evolution in front of the storm seawall is reported and discussed. In particular, bed scour at the dike toe and its evolution in terms of scour depth, width and eroded volumes are investigated. Moreover, the numerical study performed to design the experiments is illustrated, in order to analyze the performance of the model in simulating bed evolution in front of the dike in such particular foreshore conditions.

## EXPERIMENTAL SETUP

The large-scale Delta Flume is a new laboratory built in Delft to overcome difficulties due to scale effects encountered in small scale physical models (Hofland et al., 2014). It is about 300 $m$ long, 5 $m$ wide and 9.5 $m$ deep, equipped with a pyston-type wave maker able to generate extreme wave height of 4.5 $m$ with a significant wave height of 2.2 $m$. In movable bed physical models scaling issue is very important, since the downscaling of the sand particles size could alter the sediments mechanical behavior and induce a model morphodynamic feedback typical of cohesive materials (Di Risio et al., 2010). The large/full scale facilities allow to overcome these problems and correctly reproduce the morphodynamics, with reliable measurements of both suspended and bed sediment transport.

In Figure 1 a sketch of the model geometry adopted for the experiments is showed. A detailed description of the model set-up, tests program, instruments and measurements can be found in Streicher et al. (2017). In this section the experimental setup is described with particular reference to wave and morphodynamic measurements.

The initial sandy foreshore begins about 94 m from the wave paddle with a mean slope of 1/10, followed by a 1/35 sloped foreshore for 61.6 $m$, ended on a 1/2 sloped concrete dike for 1.07 $m$ with a 1/100 sloped promenade 2.35 $m$ wide. At the end of the promenade a vertical 1.6 $m$ high steel wall is realized. According to Wentworth grain size classes (Wentworth, 1922), the foreshore is constituted by a top layer ($\approx$ 0.4 m deep) of a medium sand with a $D_{50}$ equal to 0.32 $mm$ and a second layer, below the first one until the flume bottom, made of fine sand with a $D_{50}$ of 0.23 $mm$ for a total sand volume of about 1000 $m^3$.

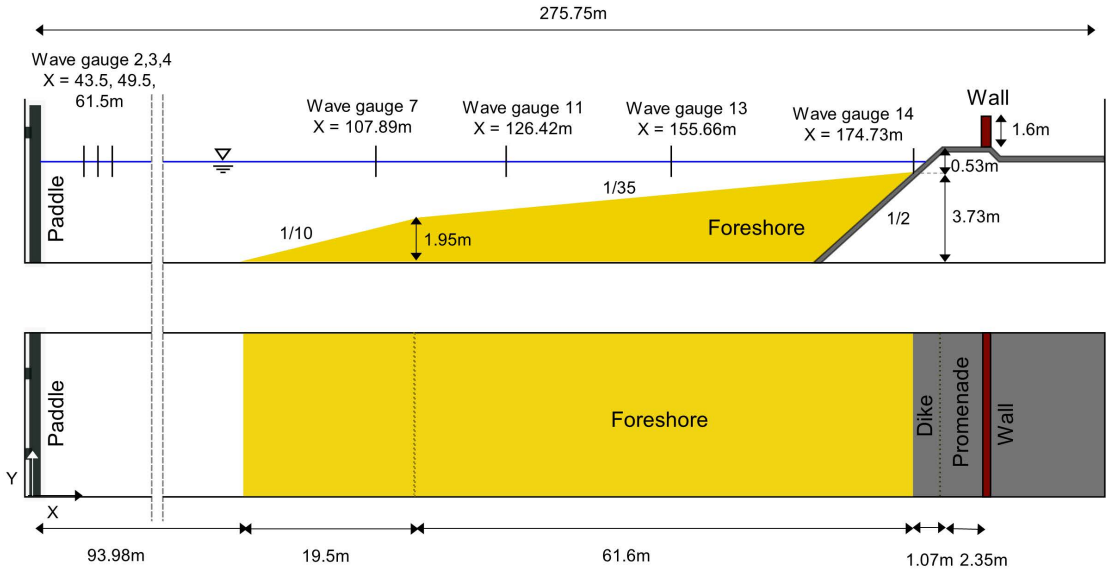


**Figure 1: Cross-section (a) and plan view (b) of the physical model built in Delta flume (from Streicher et al., 2017).**

**Table 1: Test program and main characteristics (asterisks refer to tests for which profile measurements are available).**

| testNumb | testID | n. waves | $h_0$ | $h_t$ | $H_{m0}$ | $T_{p0}$ | $T_{m-1,0}$ | $S_{p0}$ | Profile Number |
|---|---|---|---|---|---|---|---|---|---|
| - | - | - | (m) | (m) | (m) | (s) | (s) | - | - |
| | - | - | - | - | - | - | - | - | 1 (initial) |
| 1 | Bi_1_4 | ~18 | 3.99 | 0.28 | 1.12 | 6.56 | 6.69 | 0.014 | - |
| 2 | Bi_1_5* | ~18 | 4.00 | 0.29 | 1.17 | 6.78 | 6.75 | 0.015 | 2 |
| 3 | Bi_1_6 | ~18 | 4.01 | 0.30 | 1.23 | 6.86 | 7.20 | 0.016 | - |
| 4 | Bi_2_4* | ~18 | 4.13 | 0.42 | 1.15 | 6.35 | 6.31 | 0.018 | 3 |
| 5 | Irr_1_F* | ~1000 | 3.99 | 0.28 | 1.03 | 6.27 | 5.80 | 0.0175 | 4 |
| 6 | Irr_2_F* | ~3000 | 4.00 | 0.29 | 0.93 | 5.74 | 5.39 | 0.018 | 5 |
| 7 | Irr_2_S* | ~3000 | 3.99 | 0.28 | 0.93 | 5.74 | 5.38 | 0.018 | 6 |
| 8 | Irr_3_F* | ~3000 | 4.12 | 0.41 | 0.94 | 5.71 | 5.41 | 0.018 | 7 |
| 9 | Bi_2_5 | ~18 | 4.14 | 0.43 | 1.23 | 6.40 | 6.44 | 0.019 | - |
| 10 | Bi_2_6 | ~18 | 4.14 | 0.43 | 1.26 | 6.41 | 6.48 | 0.020 | - |
| 11 | Bi_2_6_R* | ~18 | 4.14 | 0.43 | 1.27 | 6.41 | 6.46 | 0.020 | 8 |
| 12 | Irr_8_F* | ~1000 | 4.13 | 0.42 | 0.52 | 4.17 | 3.89 | 0.019 | 9 |
| 13 | Irr_4_F * | ~1000 | 3.79 | 0.08 | 0.89 | 5.74 | 5.40 | 0.017 | 10 |
| 14 | Irr_5_F* | ~1000 | 3.78 | 0.07 | 1.07 | 6.27 | 5.96 | 0.017 | 11 |
| 15 | Irr_1_F_R* | ~1000 | 4.01 | 0.30 | 1.05 | 6.22 | 5.82 | 0.017 | 12 |
| 16 | Irr_7_F* | ~1000 | 4.00 | 0.29 | 0.65 | 5.03 | 4.75 | 0.016 | 13 |
| 17 | Irr_2_F_R* | ~3000 | 4.01 | 0.30 | 0.94 | 5.71 | 5.37 | 0.018 | 14 |
| 18 | Bi_1_6_R | ~18 | 4.01 | 0.30 | 1.34 | 6.34 | 6.33 | 0.021 | - |
| 19 | Bi_3_6 | ~18 | 3.77 | 0.06 | 0.99 | 6.28 | 6.77 | 0.019 | - |
| 20 | Bi_3_6_1 | ~18 | 3.77 | 0.06 | 1.07 | 6.16 | 6.94 | 0.021 | - |
| 21 | Bi_3_6_2* | ~18 | 3.76 | 0.05 | 1.19 | 7.05 | 7.13 | 0.013 | 15 |
| 22 | Irr_6_F* | ~1000 | 3.77 | 0.06 | 0.63 | 4.92 | 4.73 | 0.017 | 16 |

Irregular and bi-chromatic waves were selected as wave boundary conditions, for a total number of 22 tests. In Table 1 tests are listed in chronological order with the relative main characteristics. In particular, the test number (*testNumb*), test name (*testID*), the number of waves (*n. waves*), the water level at the wave paddle ($h_0$) and at dike toe ($h_t$), the offshore significant wave height ($H_{m0}$), peak period ($T_{p0}$), energy period ($T_{m-1,0}$) and mean wave steepness ($S_{p0}$) are reported. The bottom profiles were measured for the sea state marked by an asterisk in the column *testID*. The profile number is reported in the column *Profile Number*. Some of the reproduced sea state (11, sea states with *testID* starting with *Irr* in Table 1) consisted of irregular wave trains. They were characterized by standard JONSWAP spectrum and aimed at reproducing the 1/1000 and 1/17000 design storm conditions for the Belgian coast (Veale et al., 2012). Wave conditions for the other 11 tests consisted of bi-chromatic waves (*Bi*) for the analysis of wave-wave interaction. Besides, sea level rise has been accounted for, by testing different water levels for both irregular and bi-chromatic wave boundary conditions.

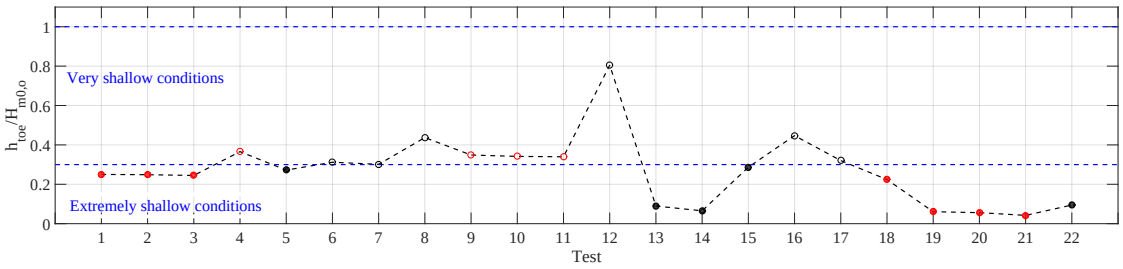


**Figure 2: Foreshore conditions for WALOWA tests, according to literature classification (e.g., Hofland et al., 2017) (red and black circles refer to bi-chromatic and irregular tests, respectively).**

The foreshore conditions, typically classified according to wave steepness or surf-similarity parameter $\xi$ (Van der Meer et al., 2016), are here evaluated by referring to the foreshore *shallowness*, namely the

water depth at toe of structure $h_t$ normalized by the offshore spectral wave height $H_{m0,o}$ (e.g., Hofland et al., 2017). Specifically, very shallow to extremely shallow foreshore are defined as $0.3 < h_t/H_{m0,o} < 1$ and $h_t/H_{m0,o} < 0.3$, respectively (Figure 2). From Figure 2 it can be confirmed that all tests were performed in very shallow to extremely shallow conditions, since the ratio $h_t/H_{m0,o}$ is less than 1 and, in particular, ranges from 0.06 up to 0.8.

Water surface elevations were measured offshore and along the foreshore until the dike toe by 7 resistance wave gauges ($WG$) deployed on the flume wall at an acquisition frequency of 1000 $Hz$. Raw surface elevation data are post-processed adopting a low-pass filtering with a cut-off frequency of 2 Hz in order to obtain the main characteristics for each test. The three wave gauges placed near the paddle are used to perform the reflection analysis by the standard method of Mansard and Funke (1980), whereas the other gauges are used to analyze waves transformation until the dike toe.

Cross-shore bed profile was measured by means of a mechanical profiler before and after 16 tests (see asterisks in Table 1). Five section were considered, along the centreline and at 0.2 $m$ and 0.4 $m$ on both sides. The mechanical profiler (Figure 3), developed by Deltares, consisted of a wheel which was attached to a measurement hinge/arm fixed to the measurement carriage, moving in both long-shore and cross-shore directions. The wheel, with a diameter equal to 10 $cm$, was able to measure the bed profile by moving with a low and constant velocity along the selected section. Both cross-shore distances and relative bed elevations were acquired. The location in $x$ direction was determined by using a laser distance meter targeting to a fixed point at the end of the flume. After each test, the foreshore was not restored to its initial configuration. Analyses are, indeed, performed by comparing the measured initial and final profiles.

**Figure 3: Mechanical profiler**

## EXPERIMENTAL RESULTS

### Hydrodynamics

Free surface elevations measured by means of wave gauges were used to estimate wave propagation along the channel from the wave paddle up to the dike toe. In Figure 4, the spatial variation of the main wave characteristics reported in Table 1 are shown for tests $Bi$ and $Irr$.

Significant wave height ($H_{m0}$) remains quite constant for irregular tests until the sandy foreshore begins. Then the waves heights are affected by restricted depth-to-height ratio and wave breaking. Along the foreshore it increases, reaching its maximum on 1/35 sloped foreshore at about 126 $m$ from the wave paddle, at the first incipient breaking section, and then it decays up to the dike. Bi-chromatic significant wave heights show small variations, with a maximum significant wave height value, for some tests, before the section depicted for the irregular wave (estimated between WG4 and WG7) and at the same section of irregular tests for others. This means that breaking section varies among the tests.

For both kind of wave boundary conditions, the cross-shore spatial distribution of the maximum relative wave height, $\gamma = H_{m0}/d$ (where $d$ is the local water depth to the still water level evaluated from measured bottom elevations) (e.g. Saponieri et al., 2018), shows a double-peak distribution for every wave conditions, as observed in Alsina et al. (2016), with maximum values along the foreshore and close to the dike toe. A

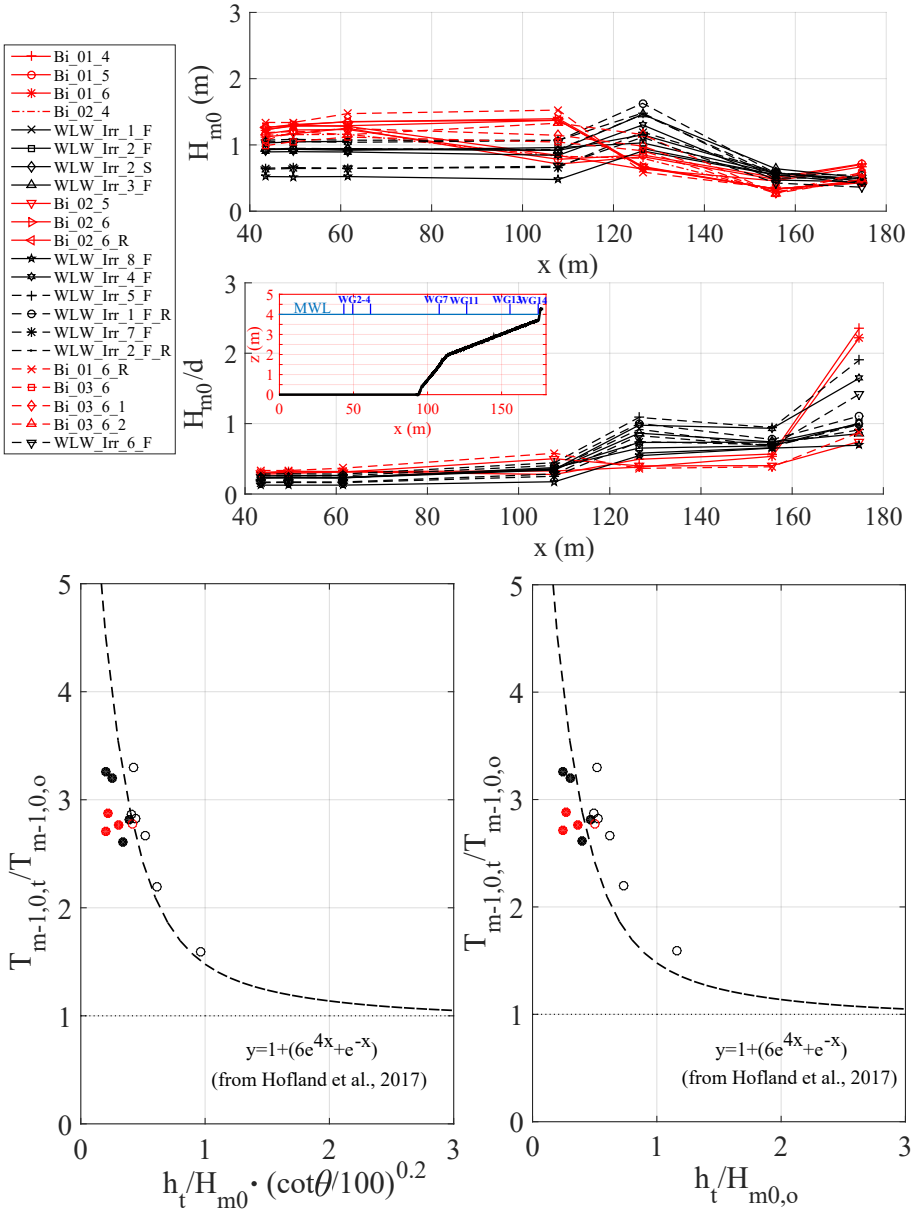


**Figure 4: Spatial variation of significant wave height ($H_{m0}$), peak period ($T_p$), energy period ($T_{m-1,0}$), wave steepness ($S_p$) and $\gamma$ distribution ($\gamma = H_{m0}/d$) versus cross-shore location for both bi-chromatic (red curves) and irregular (black curves); evolution of wave period $T_{m-1,0,t}$ as function of shallowness parameter $h_t/H_{m0,o}$ and relative water depth, according to Hofland et al. (2017).**

relative $\gamma$ peak can be observed at the same location of the maximum significant wave height, along the $1/35$ foreshore, at the section where the first breaking occurs. After primary wave breaking, $\gamma$ values decreases due to a reduction of the wave heights. At about 157 $m$ it increases, reaching the maximum at dike toe, due to small water depths despite a reduction of the wave height occurs. The maximum $\gamma$ value indicates the location of the secondary wave breaking.

Such a behaviour can be observed for all irregular tests, since any substantial changes of the bottom occurred. For bi-chromatic tests the first breaking, as estimated by the wave height spatial distribution, occurs before the first wave breaking in irregular tests. As expected, higher values of $\gamma$ are found for tests with lower water levels.

Figure 4 also reports the offshore/toe spectral period ratio as a function of the foreshore shallowness ($h_t/H_{m0}$) and the new shallowness parameter introduced by Hofland et al. (2017), i.e. $h_t/H_{m0}(cotg\theta/100)^{0.2}$. Symbols are consistent with those reported in Figure 2, where black and red circles refer to irregular and bi-chromatic tests, respectively. Filled symbols refer to tests performed in extremely shallow water condition, whereas empty ones refer to very shallow conditions. The local water depth at the structure toe was evaluated from the local bottom elevation at $WG14$ at the beginning of each test, for which the initial profile was available (15 tests).

The energy period does not remain constant during wave propagation along the foreshore and the ratio reaches a maximum value equal to 3.4 at the the lowest value of shallowness (close to zero). The dotted curve refers to the empirical formulation proposed by Hofland et al. (2017), showing a quite good agreement for WALOWA tests, especially for irregular tests performed in very shallow water conditions (black unfilled circles). The effect of mean foreshore slope ($\theta$) in the evolution of the energy period with respect to the relative water depth is less pronounced than showed by Hofland et al. (2017).

#### Morphodynamics

Morphodynamic evolution of beach profile is hereafter discussed in terms of scour formation at the dike toe induced by different wave conditions tested during WALOWA experiments (see Table 1).

In previous laboratory experiments on scour processes at coastal structures (often small-scale), the time to reach an equilibrium depth (suitable for evaluating the maximum scour) was generally very long. For example, more than 1000 waves with $H < 0.1$ $m$ and $T < 3$ $s$ were used in Sumer and Fredsøe (2000). Instead, with reference to WALOWA tests timetable, there was a temporal mixing between bi-chromatic and irregular waves, not suitable for studying long-term morphodynamics. The analyses of bed profiles refers, indeed, to transient conditions. Specifically, the study aims at evaluating the scour geometry evolution due to the variability of input wave forcing and geometrical parameters (e.g., bed slope or water depth at the dike toe) at the end of each single test.

Figure 5 reports an example of beach profile evolution evaluated at the central flume section, for 3 bi-chromatic and 1 irregular tests. Moreover, for a seek of clarity, in the same Figure 5, the sketch of the scour and the main geometrical parameters used for the analyses are reported. In the following, $S$ $(m)$ and $L_s$ $(m)$ refer to the maximum scour depth from the initial profile (scour trough) and its horizontal extension, respectively, $A_e$ $(m^2)$ is the scour area, $D_d$ $(m)$ is the distance of the scour thought from the dike toe, $\beta$ indicates the bed slope, $d$ $(cm)$ is the initial offshore water depth.

Figure 6 reports the scour temporal evolution in terms of maximum ($S$), mean depth ($\Delta z_{mean}$), length ($L_{scour}$) and volume ($V_{scour}$). The scour depth is here reported with respect to the initial profile measured before the experiments.

In general, a quantitative assessment of the parameters linked to scour processes can be highlighted as well as a rough estimate of the maximum scour process equal about to 0.3 m at WALOWA laboratory scale, corresponding to a prototype depth of about 1.3 m. The velocity of erosion process at the dike toe is higher at the beginning of the experiments, mainly during irregular waves attacks. Then, the velocity decreases and, despite the mixing of different kind of wave attacks, under both irregular and bi-chromatic waves, the scour geometry reaches a quasi-equilibrium condition, yet visible after 11 $h$ of waves. The final area interested by the scour is 9 $m$ long, has a relative mean scour depth of 0.2 m and the eroded volume is about 8 $m^3$.

In Figure 7 the dimensionless maximum scour ($S/H_{rms0}$) is reported as a function of the offshore water depth ($h_0$) normalized with respect to the wave length ($L_{p0}$) relative to the peak period ($T_p$), for two time sequences of irregular tests (from $Irr$–1–$F$ to $Irr$–3–$F$ and from $Irr$–8–$F$ to $Irr$–2–$F$–$R$, see Table 1). The values calculated by means of the empirical formulations proposed by Xie (1981) for suspension mode

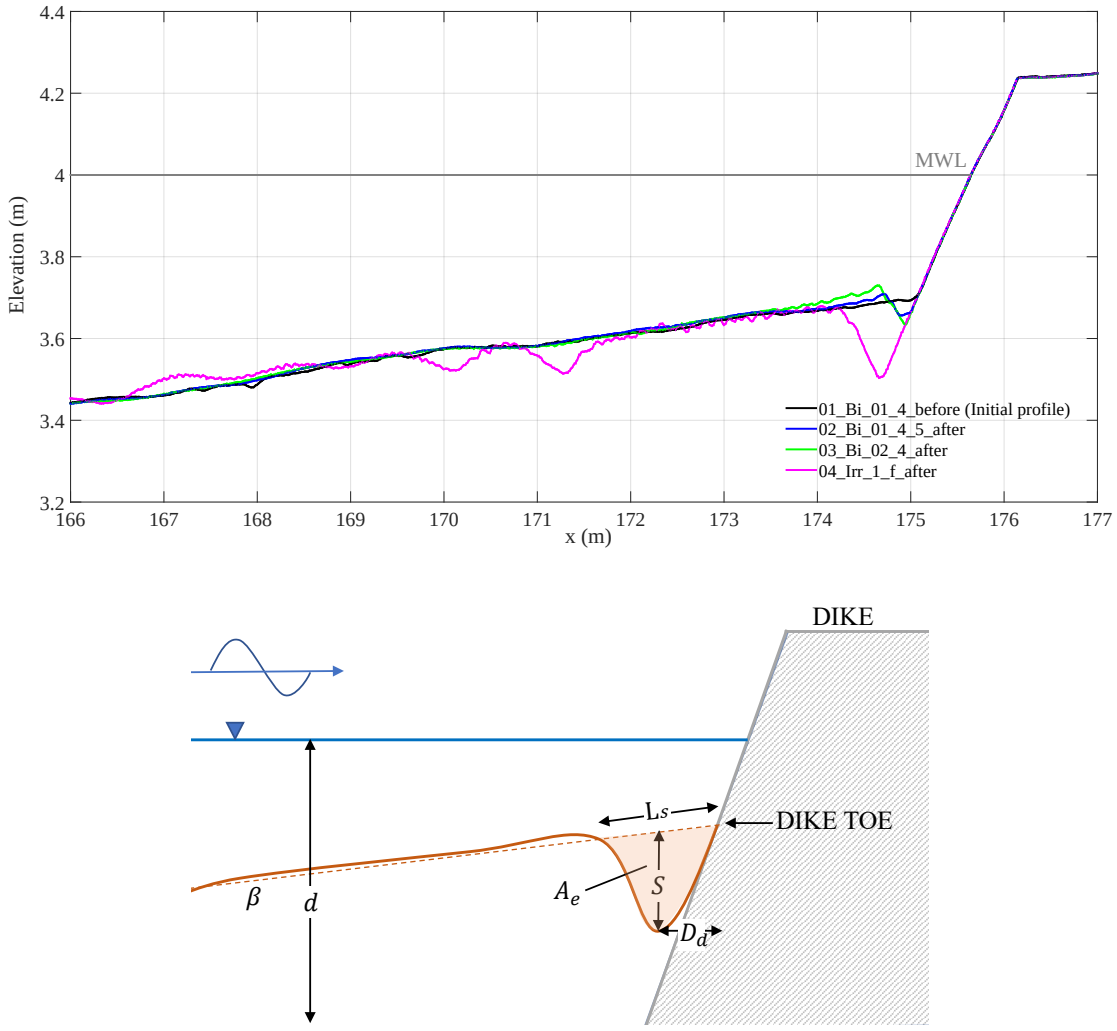


**Figure 5: Upper panel: example of bottom evolution for the first 4 tests; lower panel: sketch of parameters definition for scour.**

and Sumer et al. (2001) for coarse sand are also reported. In such formulations the maximum scour depth depends on offshore root mean square wave height ($H_{rms0}$), wave number ($2\pi/L_{p0}$) and, specifically, in Sumer et al. (2001) also on the slope of the structure, here rounded to 30°. Moreover, the formulas refer to specific boundary wave conditions. For this reason, in order to link wave characteristics to scour behaviour and compare results with the empirical formulations, the scour is calculated here with respect to the initial profile at the beginning of each single test considered.

It can be observed that measured scours range between values derived by both empirical formulations. Specifically, the formulation of Sumer et al. (2001) tends to underestimate the experimental results, especially considering that measured scours refer to transitory conditions, not comparable with the time scale of scour process. Conversely, the equation given by Xie (1981) generally overestimates the present laboratory data.

## THE NUMERICAL MODEL

In the present work, numerical modeling was employed in two steps. First, the XBeach model (Roelvink et al., 2010) was used to design the experimental investigation. Then, the same model was used to reproduce the observed bottom evolution. In the following, the two modeling steps are detailed.

In order to design the experiment, a series of preliminary numerical simulations were performed to gain insights into the evolution of the foreshore and estimate the expected amount and location of ero-

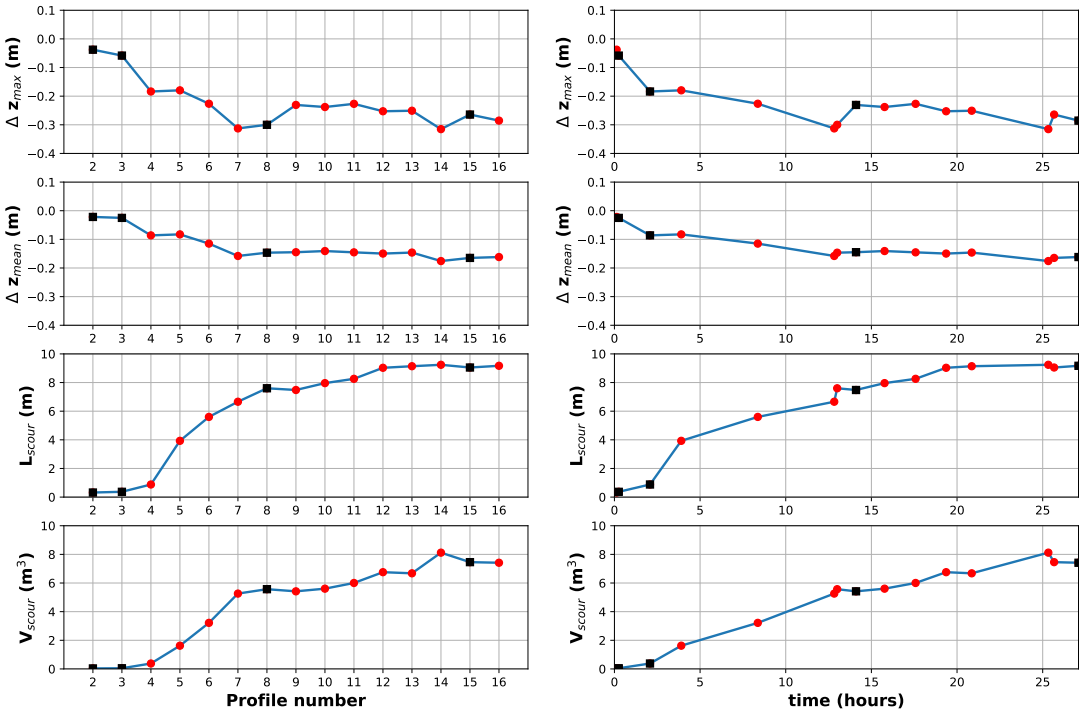


**Figure 6: Temporal evolution of scour depth ($S$), mean depth ($\Delta z$), length ($L_{scour}$) and volume ($V$). Black squares refer to bi-chromatic sea states. Profile numbers are reported in Table 1.**

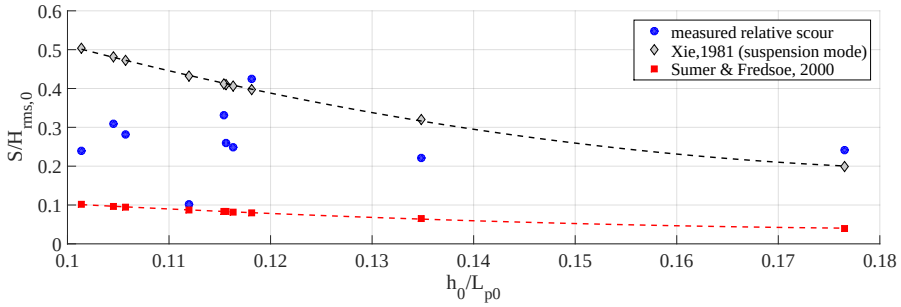


**Figure 7: Dimensionless maximum scour ($S/H_{rms0}$) versus the offshore water depth ($h_0$) normalized with respect to the wave length ($L_{p0}$).**

sion/accretion. At this step, the results cannot be validated against the observations. Figure 8 shows a sketch of the computational domain employed for the numerical simulations.

A sensitivity analysis of the model morphodynamics predictive skill was firstly performed by varying the grid spatial discretization and the boundary conditions. The simulations were carried out by imposing both stationary wave boundary conditions (hereinafter referred as STAT) and wave groups based on JONSWAP spectra (hereinafter referred as VAR). The latter, unlike the STAT condition, considers the effects induced by wave-groups and infragravity waves. For a more detailed description of the model the readers may refer to Roelvink et al. (2010). The offshore and inshore boundary conditions were set absorbing and impermeable. The duration of each simulation was selected to be equal to the (foreseen at this step) experimental one. Only for wave groups simulations (VAR) a 15 minutes warm-up interval was used during which the whole domain was considered as a fixed bottom.

Table 2 reports the main parameters of the numerical simulations. The tests sequence does not exactly match the actual test program (i.e. Table 1), as the first step of the simulations was performed to design

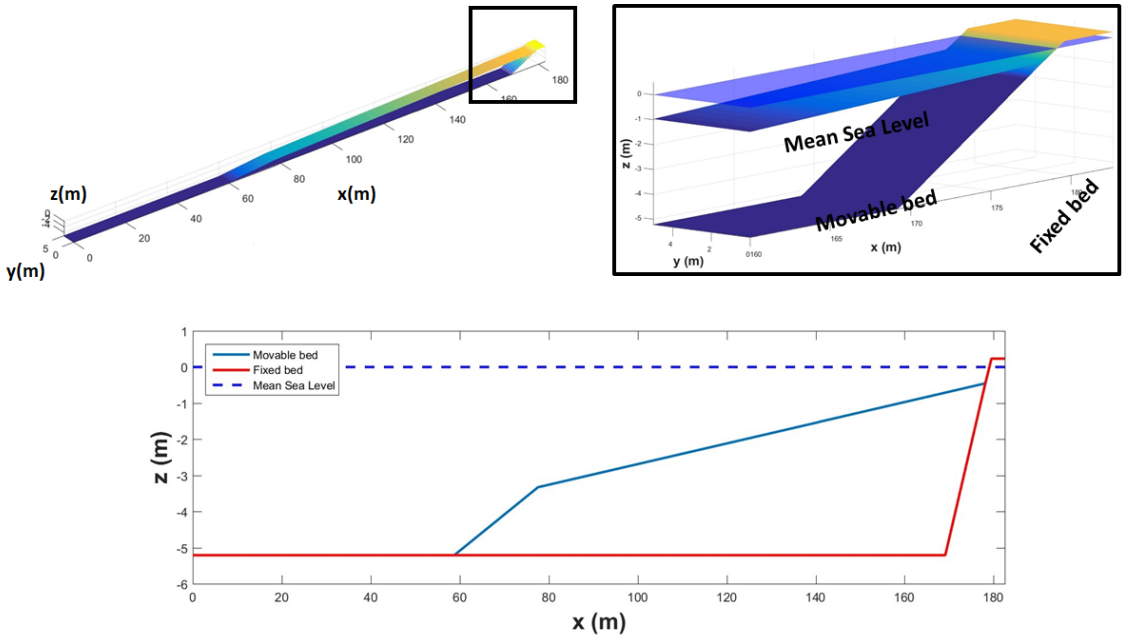


**Figure 8: Skecth of the computational domain. The upper panel shows the 2D domain and a zoom in the promenade and vertical wall area while the lowe panel show a section at y = 2,5m.**

**Table 2: Test programm related to the numerical simulation carried out to design the experiment.**

| Simulation | $H_{s-paddle}$ (m) | $T_p$ (s) | $h_{paddle}$ (m) | Duration (min) | | Sea State | B.C.(front and back) |
|---|---|---|---|---|---|---|---|
| | | | | EXP | SIM | | |
| **MB_1** | 1.21 | 6.61 | 5.21 | 110 | 110 | STAT | Absorbing (2D) |
| **MB_1** | 1.21 | 6.61 | 5.21 | 110 | 110 | STAT | Absorbing (2D) |
| **MB_1** | 1.21 | 6.61 | 5.21 | 110 | 125 (110+15) | VAR | WALL |
| **MB_2** | 1.45 | 7.24 | 5.31 | 121 | 121 | STAT | Absorbing (2D) |
| **MB_2** | 1.45 | 7.24 | 5.31 | 121 | 121 | STAT | WALL |
| **MB_2** | 1.45 | 7.24 | 5.31 | 121 | 136 (121+15) | VAR | Absorbing (2D) |
| **MB_3** | 1.21 | 6.61 | 5.21 | 331 | 331 | STAT | Absorbing (2D) |
| **MB_3** | 1.21 | 6.61 | 5.21 | 331 | 331 | STAT | WALL |
| **MB_3** | 1.21 | 6.61 | 5.21 | 331 | 346 (331+15) | VAR | Absorbing (2D) |

the experimental investigation and predict the scour and the deposition volumes. Hence, variation in test program was of course expected.

Figure 9 shows an example of the bed evolution (upper panel) and the magnitude of the scour (lower panel) computed for the test $MB_1$ with different grid sizes and boundary conditions. It can be observed that the results slightly differ for all the tested model configurations. This can be quantified by looking at Table 3, where $x_{dep}$ is the maximum length reached by the deposition area, $x_{er}$ is the maximum length reached by the erosion area and $V_{dep}$ is the total deposition volume.

A further series of tests were performed to estimate the cumulative erosion/accretion pattern without (numerically) reprofiling at the end of each test. Also in this case, both stationary and wave group conditions were investigated. Figure 10 shows the results obtained without reprofiling using STAT (left panel) and VAR (right panel) conditions. For each case, figures show in the upper panel the comparison between initial and final profiles after each test, whereas in the lower panel the total erosion/accretion in terms of depth variations are reported. The total displaced volume was estimated to be 13÷23 $m^3$ (depending on wave groupiness) with erosion expected within about 30 m offshore the seawall (x≃177 m) and accretion

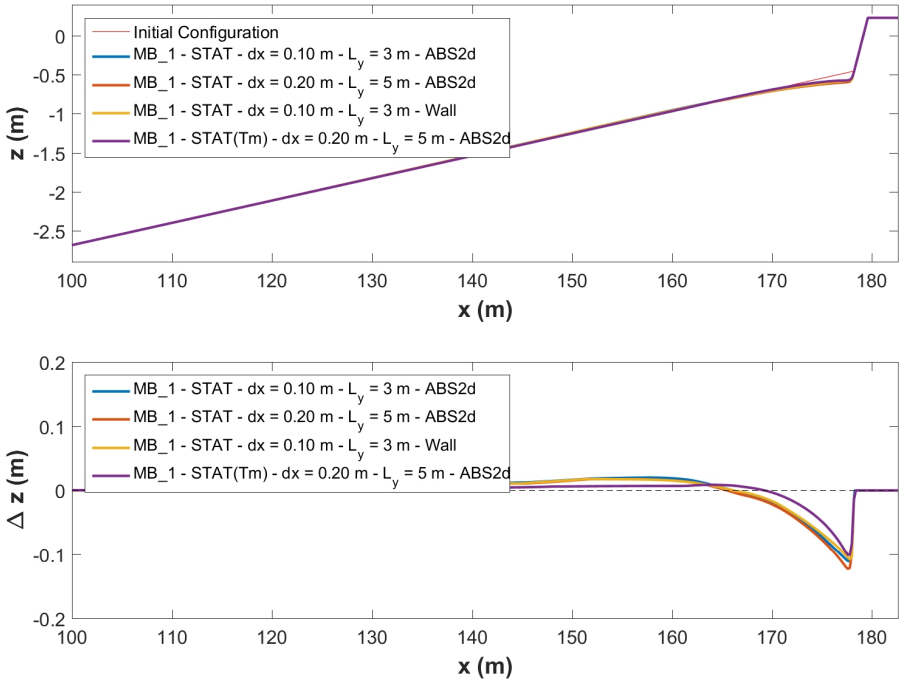


**Figure 9: Comparison between the initial configuration and the results obtained in different tests (upper panel) and the magnitude of the scour as difference between initial and final configurations (lower panel) varying the boundary conditions, the spatial discretization and the trasversal dimension of the 2D domain.**

**Table 3: Results of the sensitivity analysis carried out by varying the boundary conditions (Absorbing and Wall) and the transversal dimension $L_y$.**

| Boundary condition | $L_y$ (m) | dx (m) | $x_{dep}$ (m) | $x_{er}$ (m) | $V_{dep}$ ($m^3$) |
|---|---|---|---|---|---|
| Absorbing | 5 | 0.10 | 140.4 | 166.2 | 2.53 |
| Absorbing | 3 | 0.30 | 141.4 | 165.6 | 2.30 |
| Wall | 3 | 0.10 | 140.6 | 166.2 | 2.43 |

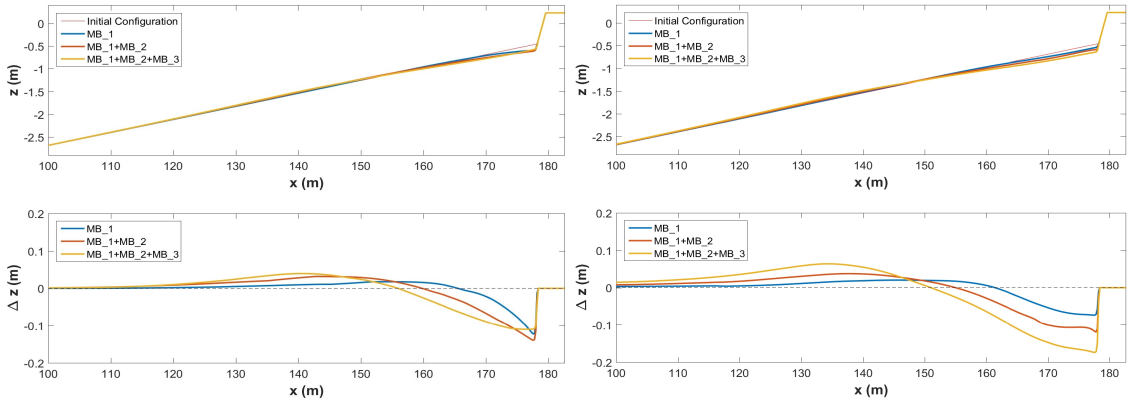


**Figure 10: Profile variations obtained without reprofiling using STAT (left panel) and VAR (right panel) conditions. For each case upper panel shows the comparison between initial and modified profile after each test while lower panel shows the total erosion/accretion in terms of depth variations**

within further 40 m.

Numerical results allowed to state that reprofiling at the end of each test was not necessary, since such small morphodynamic changes would not influence waves propagation significantly. Moreover, the sand mixing was foreseen to be not probable as the top layer of the foreshore was ≃ 0.40 m deep (see section "Experimental setup") and, hence, deeper than the predicted maximum scour.

On the basis of measurements performed during the experiments, the second step of the numerical study dealt with the validation of the XBeach model in such particular conditions, characterized by frequent occurrence of breaking waves, suspension mode of sediment transport and presence of very shallow to extremely shallow foreshore. Indeed, the test program was set equal with that detailed in Table 1. The initial configuration of the first simulation was set equal to the initial measured profile. The initial configuration of the succeeding simulations was set equal to the final (computed) configuration of the preceding run. The computed cross shore profiles were analyzed and the main parameters ($S$, $\Delta z_{mean}$) compared to the observed ones.

Figure 11 shows an example of the profile evolution during the tests. The x-label on the figure indicates the profile number (see Table 1). It is possible to observe that the model is able to catch the general trend of the scour evolution over time. Moreover, it seems to be able to correctly reproduce the magnitude of long term scour evolution (more than 18000 waves). Despite a more detailed calibration is needed in order to better reproduce the shape of the scour in front of the promenade, preliminary numerical results demonstrated the good performance of the model in predicting the overall morphodynamincs and, hence, its use as a predictive tool also in experiments design.

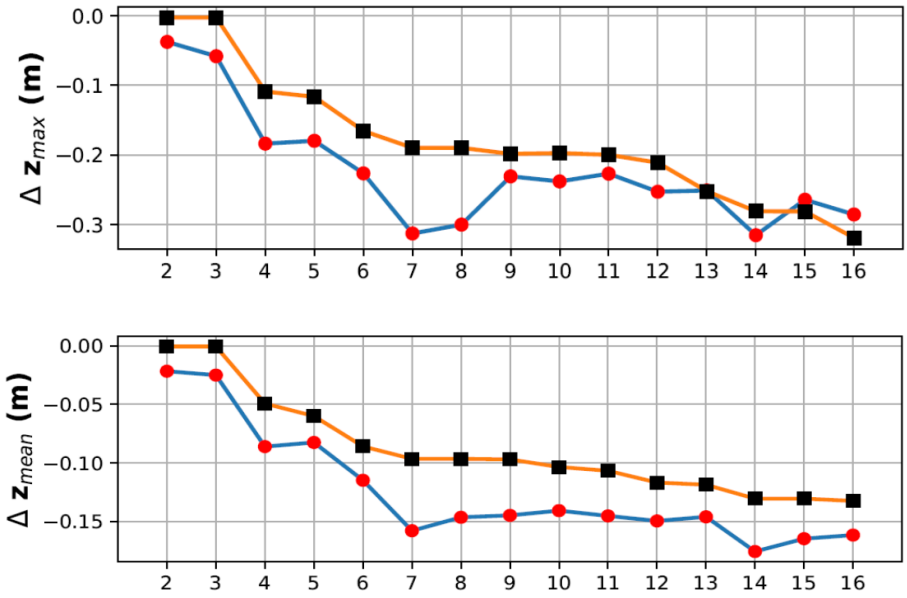


**Figure 11: Scour evolution related to test number in terms of maximum ($S$) and relative mean ($\Delta z_{mean}$) depth. The solid line with circles refers to experimental results, while the orange one with square refers to the numerical results.**

## CONCLUDING REMARKS AND ONGOING RESEARCH

In this work, experimental and numerical results of large-scale physical experiments (Froude scale, 1:4.3) performed at the new Delta Flume in 2017 are presented. Due to the presence of frequent occurrence of breaking waves, suspension mode of sediments and presence of very shallow to extremely shallow foreshore these tests represent a novelty in the field of morphodynamic effects near coastal structures for shallow foreshore.

The main investigation of the WALOWA project was aimed to quantify wave overtopping and impacts on a vertical wall placed on the top of a dike in a mildly shallow foreshore. Anyhow, a dedicated task in the project was addressed to investigate the morphological evolution of the sandy foreshore, the scour at the

dike toe and its evolution under irregular and bi-chromatic wave conditions.

XBeach model was used to perform a preliminary analysis of the evolution of the scour in order to correctly design the experiments. A sensitivity analysis was carried out by varying the boundary conditions, the 2-D domain width and the grid spatial discretization, in order to verify the influence of these parameters on the evolution of the bed layer.

Moreover, the experimental results were used as a dataset to validate XBeach in such particular conditions. The initial configuration of the first simulation was set equal to the measured profile (i.e. a mechanical profiler) and the initial configuration of the succeeding simulations was set equal to the final configuration (computed) of the preceding simulations (no reprofiling). Results show a good reliability of XBeach to reproduce the general evolution of the bed layer during the experiments and allow to have a good prediction of the general features of the scour if long time evolution is considered.

The work is still in progress with the aim to provide insight (and design criteria) about morphodynamic evolution in front of seawalls with shallow foreshore.

**ACKNOWLEDGEMENTS**

The work was supported by the European Community's Horizon 2020 Research and Innovation Programme through the grant to HYDRALAB-PLUS, Contract no. 654110. The personnel of the new Delta Flume is particularly acknowledged for their work during the experimental phase. This research was also funded by the Development Fund and Cohesion 2002-2013 APQ search Apulia Region Regional program in support of smart specialization and social and environmental sustainability-Future In Research.

**References**

W. Allsop, T. Bruce, T. Pullen, and J. Van der Meer. Direct hazards from wave overtopping-the forgotten aspect of coastal flood risk assessment? In *43rd Defra Flood and Coastal Management Conference, Manchester University.*, 2008.

J. M. Alsina, E. M. Padilla, and I. Cáceres. Sediment transport and beach profile evolution induced by bi-chromatic wave groups with different group periods. *Coastal Engineering*, 114:325–340, 2016.

C. Altomare, T. Suzuki, X. Chen, T. Verwaest, and A. Kortenhaus. Wave overtopping of sea dikes with very shallow foreshores. *Coastal Engineering*, 116:236–257, 2016.

D. Celli, D. Pasquali, P. De Girolamo, and M. Di Risio. Effects of submerged berms on the stability of conventional rubble mound breakwaters. *Coastal Engineering*, 136:16–25, 2018.

X. Chen, B. Hofland, C. Altomare, T. Suzuki, and W. Uijttewaal. Forces on a vertical wall on a dike crest due to overtopping flow. *Coastal Engineering*, 95:94–104, 2015. ISSN 03783839. doi: 10.1016/j.coastaleng.2014.10.002.

X. Chen, B. Hofland, and W. Uijttewaal. Maximum overtopping forces on a dike-mounted wall with a shallow foreshore. *Coastal Engineering*, 116:89–102, 2016.

A. De Best and E. W. Bijker. Scouring of a sand bed in front of a vertical breakwater. *Oceanographic Literature Review*, page 160, 1971. ISSN 0169-6548. URL `http://yadda.icm.edu.pl/yadda/element/bwmeta1.element.elsevier-53108313-5014-3edc-a122-79d6095efde1`.

M. Di Risio, I. Lisi, G. M. Beltrami, and P. De Girolamo. Physical modeling of the cross-shore short-term evolution of protected and unprotected beach nourishments. *Ocean Engineering*, 37(8-9):777–789, 2010.

M. Di Risio, A. Bruschi, I. Lisi, V. Pesarino, and D. Pasquali. Comparative analysis of coastal flooding vulnerability and hazard assessment at national scale. *Journal of Marine Science and Engineering*, 5(4), 2017.

J. E. Fowler, S. A. Hughes, L. A. Barnes, J. E. Evans, J. A. Denson, and R. R. Sweeney. Scour Problems & Methods for Prediction of Maximum Scour at Vertical Seawalls. *Final Report*, (December):1–46, 1992.

B. Hofland, I. Wenneker, and M. V. Gent. Description of the new delta flume. In *From Sea to Shore–Meeting the Challenges of the Sea: (Coasts, Marine Structures and Breakwaters 2013)*, pages 1346–1355. ICE Publishing, 2014.

B. Hofland, X. Chen, C. Altomare, and P. Oosterlo. Prediction formula for the spectral wave period Tm-1,0on mildly sloping shallow foreshores. *Coastal Engineering*, 123:21–28, 2017. ISSN 03783839. doi: 10.1016/j.coastaleng.2017.02.005.

E. P. Mansard and E. Funke. The measurement of incident and reflected spectra using a least squares method. In *Coastal Engineering 1980*, pages 154–172. 1980.

A. Pagano, I. Pluchinotta, R. Giordano, and U. Fratino. Integrating hard and soft infrastructural resilience assessment for water distribution systems. *Complexity*, 2018, 2018.

D. Pasquali, M. Di Risio, and P. De Girolamo. A simplified real time method to forecast semi-enclosed basins storm surge. *Estuarine, Coastal and Shelf Science*, 165:61–69, 2015.

D. Roelvink, A. Reniers, A. Van Dongeren, J. Van Thiel de Vries, J. Lescinski, and R. McCall. Xbeach model description and manual. *Unesco-IHE Institute for Water Education, Deltares and Delft University of Tecnhology. Report June*, 21:2010, 2010.

A. Saponieri, N. Valentini, M. Di Risio, D. Pasquali, and L. Damiani. Laboratory investigation on the evolution of a sandy beach nourishment protected by a mixed soft-hard system. *Water (Switzerland)*, 10 (9), 2018.

M. Streicher et al. Walowa (wave loads on walls)-large-scale experiments in the delta flume. In *SCACR2017*, pages 69–80, 2017.

B. M. Sumer and J. Fredsøe. Experimental study of 2D scour and its protection at a rubble-mound breakwater. *Coastal Engineering*, 40(1):59–87, 2000. ISSN 03783839. doi: 10.1016/S0378-3839(00)00006-5.

B. M. Sumer, R. J. Whitehouse, and A. Tørum. Scour around coastal structures: a summary of recent research. *Coastal Engineering*, 44(2):153–190, 2001.

C.-P. Tsai, H.-B. Chen, and S.-S. You. Toe Scour of Seawall on a Steep Seabed by Breaking Waves. *Journal of Waterway, Port, Coastal, and Ocean Engineering*, 135(2):61–68, 2009. ISSN 0733-950X. doi: 10.1061/(ASCE)0733-950X(2009)135:2(61).

N. Valentini, A. Saponieri, and L. Damiani. A new video monitoring system in support of coastal zone management at apulia region, italy. *Ocean & Coastal Management*, 142:122–135, 2017.

J. Van der Meer, N. Allsop, T. Bruce, J. De Rouck, A. Kortenhaus, T. Pullen, and B. Zanuttigh. Eurotop 2016: Manual on wave overtopping of sea defences and related structures. an overtopping manual largely based on european research, but for worldwide application, 2016.

W. Veale, T. Suzuki, T. Verwaest, K. Trouw, and T. Mertens. Integrated Design of Coastal Protection Works for Wenduine, Belgium. *Coastal Engineering Proceedings*, pages 1–10, 2012.

C. K. Wentworth. A scale of grade and class terms for clastic sediments. *The journal of geology*, 30(5): 377–392, 1922.

S. Xie. Scouring patterns in front of vertical breakwaters and their influences on the stability of the foundation of the breakwaters. 1981.